[5]R. H. Heist and F. K. Fong, Phys. Rev. B 1, 2970 (1970).

[6]F. K. Fong, R. H. Heist, C. R. Chilver, J. C. Bellows, and R. L. Ford, J. Luminescence 1, 823 (1970).

[7]F. K. Fong and J. C. Bellows, Phys. Rev. B 1, 4240 (1970).

[8]W. E. Bron and W. R. Heller, Phys. Rev. 136, A1433 (1964).

[9]F. K. Fong and E. Y. Wong, in *Optical Properties of Ions in Crystals*, edited by H. M. Crosswhite and H. W. Moos (Interscience, New York, 1967), p. 137.

[10]F. K. Fong, J. A. Cape, and E. Y. Wong, Phys. Rev. 151, 299 (1966).

[11]M. Tinkham, *Group Theory and Quantum Mechanics* (McGraw-Hill, New York, 1964), Chap. 5.

[12]These values are actually calculated for the NaCl:Sr^{2+} system. F. Bassani and F. G. Fumi, Nuovo Cimento 11, 274 (1954); M. P. Tosi and G. Airoldi, *ibid.* 8, 584 (1958).

[13]G. D. Watkins, Phys. Rev. 113, 79 (1959); 113, 91 (1959).

PHYSICAL REVIEW B VOLUME 2, NUMBER 7 1 OCTOBER 1970

Behavior of Helical Spin Structures in Applied Magnetic Fields

J. M. Robinson and Paul Erdös

Department of Physics, The Florida State University, Tallahassee, Florida 32306

(Received 11 May 1970)

The problem of the behavior of helical spin structures and the phase transitions they exhibit in applied magnetic fields is studied theoretically. We have obtained a numerical solution valid for the planar helix at $T=0$ °K with an arbitrary number of interplanar exchange interactions, an arbitrary form of in-plane anisotropy, and an external magnetic field applied in the plane. We calculated the phase diagram for the case of two interplanar exchange constants and no anisotropy, and found different behavior in the intermediate field region from that predicted by the previous theory. As a new result, in the case of an in-plane anisotropy, the angle dependence of the transition fields has been obtained.

I. INTRODUCTION

A large number of materials are known, such as the rare-earth metals Tb,[1] Dy,[1] Ho,[1] Eu,[2] and the manganese compounds MnO_2,[3] $MnAu_2$,[4] and MnP,[5] which exhibit planar helical spin structures below the ordering temperature T_N. The model which is invoked to describe this situation is that of a succession of exchange-coupled ferromagnetic layers with the moment of a given layer lying in the plane of the layer. If the competing interlayer exchange constants are of sufficient magnitude, the classical ground state may be shown to be a spiral (helix), in which the angle between the magnetic moments of two consecutive layers is a constant q_0.

When an external magnetic field is applied parallel to the plane of the helix, transitions to other types of spin structures can be induced, resulting in discontinuities in the net magnetization and in the susceptibility. Nagamiya *et al.*[6] and Herpin *et al.*[7] have developed an approximate analytic theory for the planar spiral by series expansions. In weak fields the energy of the spin system is developed in powers of the applied field, assuming that the deviations of the spins from their directions in zero field are small. High field solutions are obtained by expanding the energy in powers of the angles of deviation of the spins from the field direction. The fields at which transitions between low and high field solutions, i.e., between two phases, occur were obtained by extending the curves which represent the energy as a function of the magnetic field to their intersection in intermediate fields. When there is anisotropy in the plane, this theory has been worked out in the special case of the magnetic field applied along a symmetry axis.[8] The preceding theory and its molecular field generalization to finite temperatures[8] have had wide application, but because of the approximations made, its validity for intermediate fields was not known. A more exact treatment is therefore needed.

We present here a numerical solution for a planar spiral at $T=0$ °K, whose axis of rotation is normal to the planes, with an arbitrary *in-plane anisotropy* and an *external field* applied in the plane at an arbitrary angle with respect to the in-plane anisotropy axes. The spins are assumed to be always constrained to the plane of the layers, as, for example, in the typical case of a strong

out-of-plane anisotropy. The method will, in principle, handle any number of interlayer exchange constants, but the present calculations are limited to the case of exchange constants α_1 and α_2 between first- and second-nearest-neighbor layers, respectively. We describe applications to experimental bulk magnetization measurements.

II. NUMERICAL METHOD

We first consider the mathematical model of a "unit cell" of *N layers of spins*, each spin of *magnitude S*. Since all spins in one layer are parallel to each other, their exchange interaction is not a variable and need not be considered. Therefore, the "unit cell" will contain only one spin per layer. Periodic boundary conditions are applied, making the *periodicity q* a rational multiple of 2π. The *average energy per spin E* of this system is

$$E=\frac{1}{N}\sum_{j=1}^{N}\{\alpha_1\cos(\phi_{j+1}-\phi_j)+\alpha_2\cos(\phi_{j+2}-\phi_j) - \mu_B gSH\cos(\phi_j-\phi_0)-\mu_B gSH_A\cos n_A\phi_j\}, \tag{1}$$

where $\alpha_1(\alpha_2)$ is the exchange constant to the first-(second-) nearest-neighbor layer, H is the external magnetic field applied at an angle ϕ_0 relative to an arbitrarily chosen axis of minimum in-plane anisotropy (an "easy axis"), ϕ_j is the angle the spin the jth layer makes with this axis, and H_A is the anisotropy field of multiplicity n_A(n_A-fold anisotropy axis). The boundary conditions require $\phi_{N+j}=\phi_j$ for all j.

For given initial values of the N variables ϕ_j one solves the N coupled transcendental equations

$$\frac{\partial E}{\partial\phi_i}=0,\quad i=1,2,\ldots,N \tag{2}$$

by a generalization of Newton's method.[9] This finds the local minimum of energy with respect to the variables ϕ_i nearest the initial values of ϕ_i. If H is incremented by only a small amount each time the above equations are solved, using as initial values the solution for the preceding value of H, the net magnetization and energy can be obtained numerically as a function of H for a given spin configuration (solution type) subject to the constraint of a fixed periodicity. The manifold of phases (solution types) used as initial values in the calculations is shown schematically in Fig. 1 along with the corresponding analytic expressions for the angles ϕ_n for the helix and fan. The structures are shown distorted as they would be in a finite external or anisotropy field. One has not proven that the solution of lowest energy is one of these types, but these are the only types found experimentally or theoretically under the conditions of our problem.

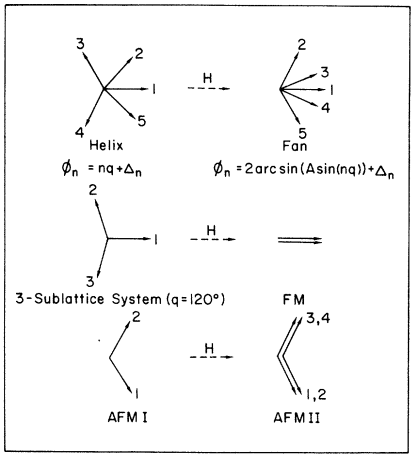

FIG. 1. Schematic representation of the various phases of a planar spiral spin arrangement in an external magnetic field applied in the plane. The expressions for ϕ_n give the corresponding analytic solution for the angle of the spin with respect to an arbitrary fixed axis parallel to the plane of the spin in the nth layer. The periodicity of the spiral is q, Δ_n is a field-induced distortion, and A is dependent on H only ($|A|<1$). The numerals on the spin vectors denote consecutive layers in one unit cell. For the helix and fan, N denotes the maximum number of layers in the unit cell. The diagram shows the example $N=5$. The abbreviations FM, AFMI, and AFMII are explained in Sec. III.

A complication which must be taken into account is that the periodicity q of the helix and fan phases is a field-dependent variable, as has been observed by neutron diffraction.[10,11] The energy must also be minimized with respect to q, and Fig. 2 outlines the basic procedure for doing this. Having fixed α_1, α_2, H_A, n_A, and ϕ_0, one determines a grid of rational values of q, $q=2\pi m/N$ (m integer), chosen to cover the region in which the periodicity is expected to vary over the range of the field H. It is found that since q is a relatively slowly varying function of H, a grid of about ten rational values yields sufficient accuracy over wide ranges of H for a given phase. Corresponding to each rational q, there is a "unit cell" of minimal m and N in which the evolution of the energy and magnetization with H may be determined as previously described. For practical use, N should be less than about 70.

The initial values for ϕ_n in each cell are obtained from the analytic expressions reproduced in Fig. 1 which can be evaluated at certain limiting values of H as follows: For the helix, at $H=0$, one has

$$q(H=0)=q_0=\arccos(-\tfrac{1}{4}\alpha_1/\alpha_2)\,. \tag{3}$$

For the fan, the solutions are started at H slightly less than the saturation field H_0 given by

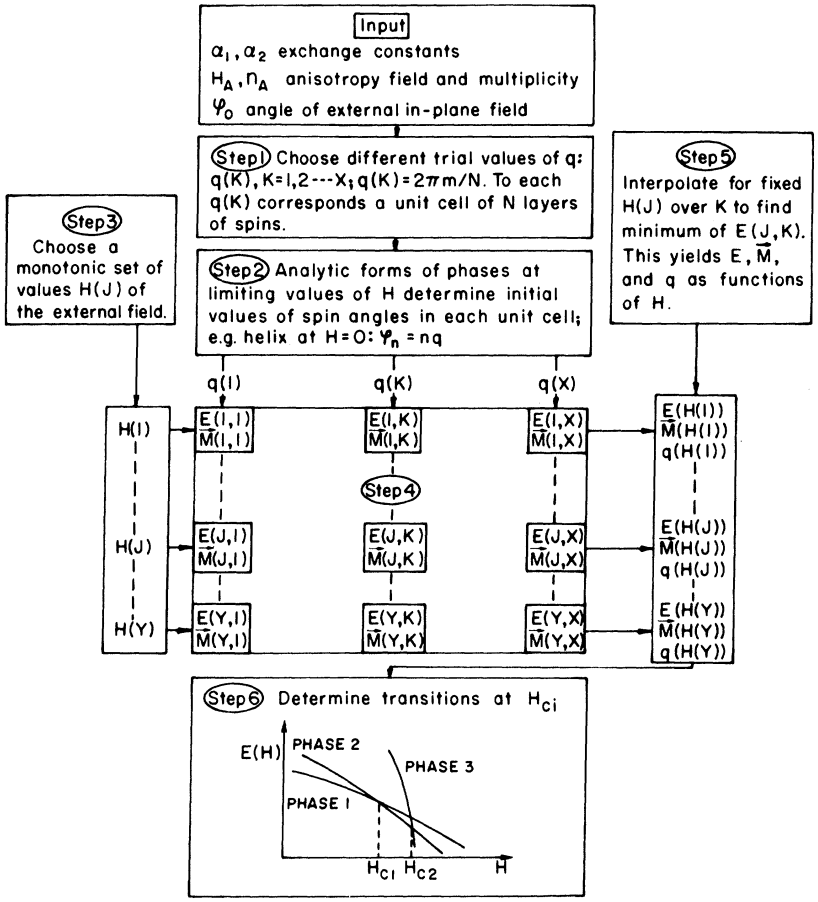

FIG. 2. Flow chart of the numerical method used to determine the behavior of a planar spiral spin structure in an external magnetic field.

$$H_0 = [J(q_0) - J(0)]/\mu_B g S \ , \tag{4}$$

with

$$J(q) = 2\alpha_1 \cos q + 2\alpha_2 \cos 2q \ . \tag{5}$$

When H approaches H_0, the fan periodicity approaches q_0, as shown analytically by Nagamiya *et al.*[6] The field is incremented (increased for the helix, decreased for the fan) in steps ΔH of the order of $\pm \frac{1}{50} H_0$ until the energy and magnetization of each unit cell are obtained for the set of field values for a given phase. For a particular value of H, the energy is found to be a smoothly varying function of q with a well-defined minimum which can now be obtained by interpolating a curve through the energy values corresponding to the grid of q values. The physical solutions for the average energy per spin E, and the relative magnetization M for the given value of H are obtained by evaluating the corresponding interpolated curves at the value of q for which E is a minimum.

Carrying out this procedure for each value of H, then, yields finally E, M, and q numerically as functions of H for a given configuration. *First-order phase transitions* (such as helix → fan) are obtained by locating the point at which the energy curves of two configurations of lowest energy cross. *Second-order phase transitions* (such as fan → ferromagnet in zero anisotropy) are obtained by locating the intersection of the corresponding magnetization curves.

III. PLANAR HELIX WITH ZERO IN-PLANE ANISOTROPY

In order to check the above method and to obtain comparisons with the previous approximate calculations of Nagamiya *et al.*,[6] we have computed the α_2/α_1, H *phase diagram* for the planar helix with no in-plane anisotropy. From the limit $H = 0$, we conclude that there are *four cases* (A, B, C, and D) to be considered, depending on the relative signs of the first and second interplanar exchange constants, α_1 and α_2. From Eq. (1) with $H = H_A = 0$ and $\phi_{i+1} - \phi_i = q$ it follows that

$$E = \alpha_1 \cos q + \alpha_2 \cos 2q \ . \tag{6}$$

By minimizing this expression with respect to q,

one finds the following stable configurations in zero external field:

A. $\alpha_1 < 0$ and $\alpha_2 < 0$, ferromagnet (FM)

B. $\alpha_1 > 0$ and $\alpha_2 < 0$, type I antiferromagnet (AFMI)

C. $\alpha_1 < 0$, $\alpha_2 > 0$: $4\alpha_2 > -\alpha_1$, helix with acute turn angle $(0 < q_0 < \frac{1}{2}\pi)$
$4\alpha_2 \leq -\alpha_1$, FM

D. $\alpha_1 > 0$, $\alpha_2 > 0$: $4\alpha_2 > \alpha_1$, helix with obtuse turn angle $(\frac{1}{2}\pi < q_0 < \pi)$
$4\alpha_2 \leq \alpha_1$, AFMI.

The designation AFMI refers to the usual *two-sublattice antiferromagnet* (each layer parallel to its second nearest neighbor). This is in contrast to AFMII, which denotes a *four-sublattice antiferromagnet* (in zero field, pairs of adjacent parallel layers with neighboring pairs antiparallel). Cases A and B above need not concern us further, since the application of an external field causes no phase changes except for the second-order AFMI → FM transition at $H = H_0$ [Eq. (4) with $q_0 = \pi$].

The numerical method described in Sec. II allows the determination of the complete phase diagram, shown in Fig. 3, starting from the four configurations found at $H = 0$ in cases C and D above. The coordinates of the phase boundaries are given in Table I. One finds very good agreement with Nagamiya *et al.*[6] for the helix with acute zero-field turn angle (lower half of diagram), but for the more complicated case of the helix with obtuse turn angle (upper half of diagram), the behavior in intermediate fields is rather different, as will be explained. The transitions fan → FM and AFMI → FM are of *second order*; all other boundaries in Fig. 3 mark *first-order* transitions except in the region surrounding the three-sublattice system, where the transitions are of *higher order*.

If the turn angle is acute and $|\alpha_2/\alpha_1|$ is not too large, increasing H from zero distorts the helix and induces a small net magnetization with a nearly constant susceptibility until a critical field is reached at which there occurs a large discontinuous jump in magnetization, from ~10% to ~90% of the saturation magnetization. This marks the well-known helix → fan transition, which has been observed in several rare-earth metals.[11] The fields required to cause transitions are relatively small compared to the exchange field, and the periodicity of the helix and fan changes very slightly (~1%) over the entire range of fields.

By contrast, for the spiral with obtuse turn angle the fields required to reach the region of transitions are generally of the order of the exchange field, and the periodicity of the helix and fan configurations changes significantly (~10%) over the intervals of H in which these phases exist. For α_2/α_1 in the neighborhood of 0.5, q approaches $\frac{1}{3}\pi$, varying roughly as the square of the field. When q reaches $\frac{1}{3}\pi$, the spins are in the *three-sublattice system*. There is no discontinuity in the magnetization, but there is a discontinuity in the derivative of q with respect to H; the susceptibility is constant in this phase. Qualitatively the behavior is as previously described by Nagamiya *et al.*,[6] but we find that the region of the three-sublattice phase is considerably reduced; and there appears in the neighborhood of $\alpha_2/\alpha_1 = 0.95$ a boundary of first-order helix → fan transitions not previously found in this region. In all cases the numerical solutions agree with the analytic approximations in the limit of high and low fields.

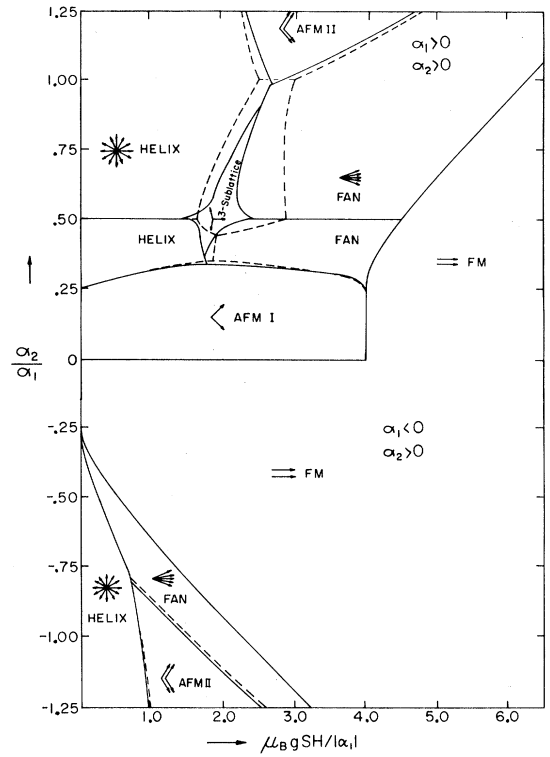

FIG. 3. Phase boundaries for a planar helix with first- and second-nearest-neighbor interplanar exchange constants α_1 and α_2. The external magnetic field H is applied in the plane. The solid line represents the numerical calculation. The dashed line represents the analytic approximation of Nagamiya *et al.* (Ref. 6).

IV. PLANAR HELIX WITH IN-PLANE ANISOTROPY

The introduction of even a small in-plane anisotropy of the order of 10^{-3} to 10^{-4} of the exchange

TABLE I. Transition fields in units of $\mu_B gSH/|\alpha_1|$ for various values of the ratio of second- to first-nearest-neighbor interplanar exchange constant α_2/α_1, for the case of the planar spiral with no in-plane anisotropy. $\mu_B gS$: magnetic moment of the ion. H: external magnetic field. The numbers in parentheses refer to the type of transition as follows: (1) helix→AFMI; (2) AFMI→fan; (3) fan→FM; (4) helix→fan; (5) helix→AFMI; (6) AFMI→fan; (7) helix→three-sublattice; (8) three-sublattice→fan; (9) AFMI→FM. See also Fig. 3.

α_2/α_1	Transition fields			α_2/α_1	Transition fields		
−1.25	0.94 (1)	2.52 (2)	3.22 (3)	0.45	1.66 (7)	1.93 (8)	4.34 (3)
−1.20	0.92 (1)	2.29 (2)	3.02 (3)	0.47	1.65 (7)	2.03 (8)	4.41 (3)
−1.15	0.90 (1)	2.08 (2)	2.82 (3)	0.49	1.60 (7)	2.19 (8)	4.47 (3)
−1.10	0.88 (1)	1.87 (2)	2.63 (3)	0.51	1.51 (7)	2.36 (8)	4.53 (3)
−1.05	0.86 (1)	1.66 (2)	2.44 (3)	0.53	1.70 (7)	2.25 (8)	4.59 (3)
−1.00	0.83 (1)	1.46 (2)	2.24 (3)	0.55	1.79 (7)	2.20 (8)	4.66 (3)
−0.95	0.80 (1)	1.26 (2)	2.06 (3)	0.57	1.84 (7)	2.20 (8)	4.72 (3)
−0.90	0.77 (1)	1.07 (2)	1.87 (3)	0.59	1.86 (7)	2.20 (8)	4.78 (3)
−0.85	0.74 (1)	0.88 (2)	1.78 (3)	0.61	1.89 (7)	2.20 (8)	4.85 (3)
−0.80	0.70 (1)	0.71 (2)	1.50 (3)	0.63	1.92 (7)	2.20 (8)	4.92 (3)
−0.75	•••	0.62 (4)	1.32 (3)	0.65	1.95 (7)	2.21 (8)	4.98 (3)
−0.70	•••	0.54 (4)	1.15 (3)	0.67	1.99 (7)	2.22 (8)	5.05 (3)
−0.65	•••	0.46 (4)	0.98 (3)	0.69	2.03 (7)	2.24 (8)	5.12 (3)
−0.60	•••	0.38 (4)	0.82 (3)	0.71	2.07 (7)	2.26 (8)	5.19 (3)
−0.55	•••	0.31 (4)	0.75 (3)	0.73	2.12 (7)	2.28 (8)	5.26 (3)
−0.50	•••	0.24 (4)	0.50 (3)	0.75	2.16 (7)	2.30 (8)	5.34 (3)
−0.45	•••	0.16 (4)	0.36 (3)	0.77	2.21 (7)	2.33 (8)	5.41 (3)
−0.40	•••	0.10 (4)	0.22 (3)	0.79	2.25 (7)	2.36 (8)	5.48 (3)
−0.35	•••	0.05 (4)	0.12 (3)	0.81	2.29 (7)	2.39 (8)	5.56 (3)
−0.30	••◦	0.02 (4)	0.04 (3)	0.83	2.34 (7)	2.42 (8)	5.63 (3)
−0.25	◦••	0.00 (4)	0.00 (3)	0.85	2.38 (7)	2.44 (8)	5.70 (3)
−0.20	•••	•••	•••	0.87	2.43 (7)	2.47 (8)	5.78 (3)
−0.15	•••	••◦	•••	0.89	2.48 (7)	2.50 (8)	5.85 (3)
−0.10	•••	••◦	•◦•	0.91	•••	2.52 (4)	5.92 (3)
−0.05	••◦	•••	•••	0.93	•••	2.56 (4)	5.99 (3)
−0.00	•••	•••	•••	0.95	•••	2.59 (4)	6.06 (3)
0.05	•••	•••	4.00 (9)	0.97	•••	2.63 (4)	6.13 (3)
0.10	◦••	•••	4.00 (9)	0.99	2.68 (1)	2.73 (2)	6.21 (3)
0.15	•••	•••	4.00 (9)	1.01	2.64 (1)	2.92 (2)	6.28 (3)
0.20	•••	•◦◦	4.00 (9)	1.03	2.61 (1)	3.11 (2)	6.36 (3)
0.25	0.00 (5)	4.00 (6)	4.00 (3)	1.05	2.58 (1)	3.28 (2)	6.43 (3)
0.27	0.25 (5)	3.94 (6)	4.01 (3)	1.07	2.54 (1)	3.45 (2)	6.50 (3)
0.29	0.53 (5)	3.82 (6)	4.02 (3)	1.09	2.51 (1)	3.61 (2)	6.57 (3)
0.31	0.88 (5)	3.41 (6)	4.04 (3)	1.11	2.48 (1)	3.77 (2)	6.64 (3)
0.33	1.42 (5)	2.41 (6)	4.07 (3)	1.15	2.45 (1)	3.91 (2)	6.71 (3)
0.35	•••	1.75 (6)	4.10 (3)	1.16	2.42 (1)	4.06 (2)	6.79 (3)
0.37	1.71 (7)	1.74 (6)	4.14 (3)	1.17	2.40 (1)	4.20 (2)	6.86 (3)
0.39	1.70 (7)	1.76 (6)	4.20 (3)	1.19	2.37 (1)	4.34 (2)	6.93 (3)
0.41	1.68 (7)	1.80 (6)	4.24 (3)	1.21	2.35 (1)	4.46 (2)	7.00 (3)
0.43	1.67 (7)	1.86 (6)	4.29 (3)	1.23	2.33 (1)	4.59 (2)	7.07 (3)

field profoundly alters the behavior described above. Because of the additional variables H_A, n_A, and ϕ_0, it is impractical to attempt a complete description of this problem. In order to illustrate the effects involved, we limit ourselves to the case of a uniaxial (twofold) anisotropy in the plane and study the dependence of the helix–AFMI (or AFMII) transition on the angle of the external field and on the magnitude of the anisotropy.

The results for a certain choice of the parameters are shown in Fig. 4. If H_A is very small ($H_A \lesssim 10^{-4} H_{\text{exchange}}$), the helix is distorted so that the spins do not uniformly cover a circle of radius S in the plane but are more concentrated in the segments of minimum anisotropy energy. For fixed α_1/α_2, the periodicity changes so as to approach π with increasing H_A, and there occurs a critical value of H_A above which the AFMI (or AFMII) phase is the state of lowest energy with the spins lying along the easy axis. The application of an external field at an angle close to the easy axis can then restore the helical phase, and at still higher fields

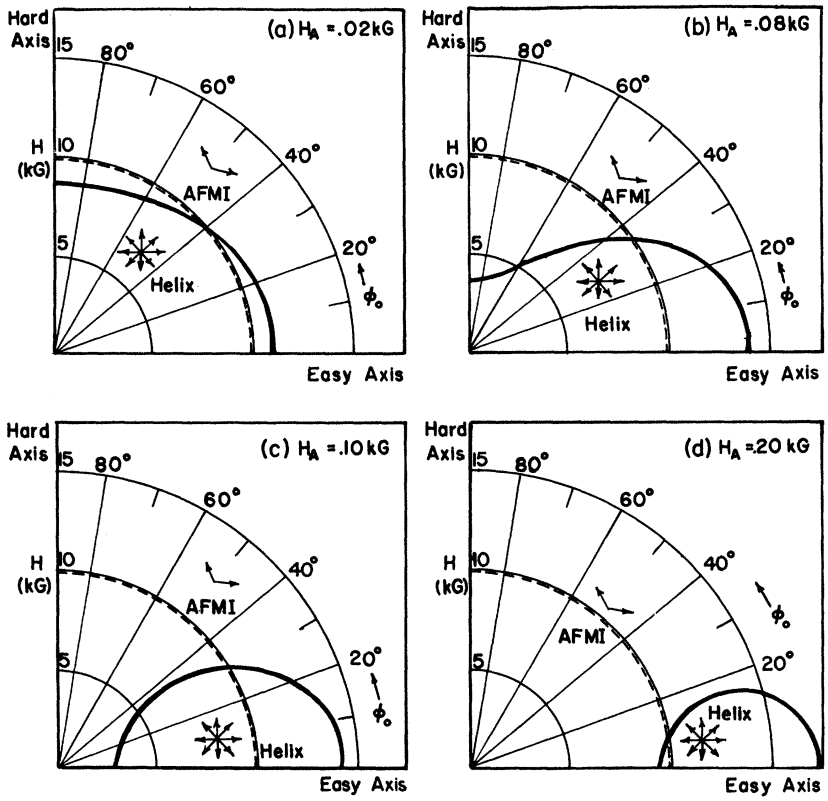

FIG. 4. Polar magnetic phase diagram of a planar spiral with uniaxial in-plane anisotropy for nearest-neighbor interplanar exchange $\alpha_1/k_B = -11.81$ °K, $\alpha_1/\alpha_2 = 0.264$ (α_2 = second-nearest-neighbor exchange), and zero-field periodicity $q_0 = 161.05°$. Solid lines: Critical field H for the *helix* → AFMI phase transitions as function of the angle ϕ_0 of the external field with respect to the easy axis. (a)–(d) are for different in-plane uniaxial anisotropy fields H_A. The dashed circle shows the transition for $H_A = 0$.

the AFMI (or AFMII) configuration returns in a "spin-flop" phase [Figs. 4(c) and 4(d)]. These are first-order transitions.

It is often the experimental case that a single crystal is not available, but that the material is in the form of platelets[12] or thin needles,[13] in either case with the c axis (normal to the plane of the helix) defined but with the in-plane axes randomly oriented in the sample. In this case, with an external field applied normal to the c axis, discontinuities in the magnetization will not in general be observed, but regions of changes in slope may be seen. The method described above can still be applied to this situation by numerically averaging the mathematical solutions for magnetization for a given $\vec{H}$ over all angles which $\vec{H}$ makes in the plane with the anisotropy axes, and a fit to the experimental data may be carried out.

Figure 5 shows the behavior of the energy and magnetization in the situation corresponding to Fig. 4(c) and illustrates the above points.

V. CONCLUSIONS

We have found that the numerical solution for the planar helix reveals different behavior in intermediate magnetic fields from that predicted by the approximate analytic solutions. The range of application of the theory of Nagamiya *et al.*[6] has been extended to include the case of in-plane anisotropy with the external field applied at an arbitrary angle with respect to the anisotropy axes, which is par-

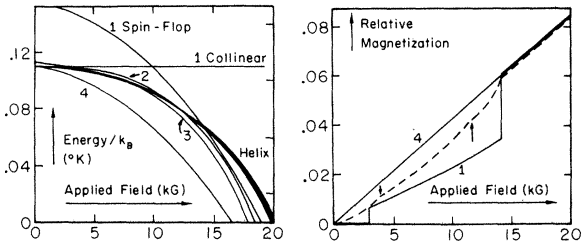

FIG. 5. Diagram of the behavior of energy and magnetization of a planar spiral spin system with in-plane uniaxial anisotropy in the case corresponding to Fig. 4(c). Upper diagram: Energy E versus applied field H of the antiferromagnetic solutions for four angles ϕ_0 of H relative to the easy axis. (1) $\phi_0 = 0$; (2) $\phi_0 = \frac{1}{12}\pi$; (3) $\phi_0 = \frac{1}{3}\pi$; (4) $\phi_0 = \frac{1}{2}\pi$. The curves for the helix are almost coincident for the four angles (1)–(4), and are shown labeled "Helix." Lower diagram: Magnetization curves for angles (1) $\phi_0 = 0$ and (4) $\phi_0 = \frac{1}{2}\pi$ (solid lines) and averaged over all angles ϕ_0 (dashed lines). The two arrows indicate the remnants of the discontinuities of the magnetization.

ticularly important for applications to experiment.

The angle dependence of transition fields can be obtained for comparison with experiments on single crystals, and if only the c axis of the sample is defined, comparisons with experiment may be made by numerical averaging of the solutions over all in-plane angles. The material VF_2,[13,14] a planar spiral with $q_0 = 96°$, should be a good subject for this type of study. High-field magnetization ($H \perp c$ axis) at $T \ll T_N = 7\,°K$ on this compound would permit an instructive application of the theory here described; behavior similar to that depicted in Fig. 4 should be found, if as reported[13] the in-plane anisotropy is uniaxial and small.

ACKNOWLEDGMENTS

Research sponsored by the Air Force Office of Scientific Research, Office of Aerospace Research, United States Air Force, under grant number AFSOR 69-1745. The numerical calculations were done by the CDC 6400 digital computer of The Florida State University, partially supported by the grant GJ 367 of the U.S. National Science Foundation.

[1]W. C. Koehler, J. Appl. Phys. 37, 1056 (1966).
[2]R. L. Cohen, S. Hüfner, and K. W. West, Phys. Rev. 184, 263 (1969).
[3]A. Yoshimori, J. Phys. Soc. Japan 14, 807 (1959).
[4]A. Herpin, P. Mériel, and J. Villain, Compt. Rend. 249, 1334 (1959); A. Herpin and P. Mériel, J. Phys. Radium 22, 337 (1961).
[5]G. P. Felcher, J. Appl. Phys. 37, 1056 (1966).
[6]T. Nagamiya, K. Nagata, and Y. Kitano, Progr. Theoret. Phys. (Kyoto) 27, 1253 (1962).
[7]A. Herpin, P. Mériel, and J. Villain, J. Phys. Radium 21, 67 (1960).
[8]Y. Kitano and T. Nagamiya, Progr. Theoret. Phys. (Kyoto) 31, 1 (1964).
[9]T. R. McCalla, *Introduction to Numerical Methods and Fortran Programming* (Wiley, New York, 1967), Chap. 3, p. 92.
[10]Y. Ishikawa, T. Komatsubara, and E. Hirahara, Phys. Rev. Letters 23, 10 (1969); 23, 532 (1969).
[11]W. C. Koehler, J. W. Cable, H. R. Child, M. K. Wilkinson, and E. O. Wollan, Phys. Rev. 158, 450 (1967).
[12]S. L. Carr, P. Erdös, W. G. Moulton, and J. Robinson, Solid State Commun. 7, 1673 (1969).
[13]J. W. Stout and H. Y. Lau, J. Appl. Phys. 38, 3 (1968); 38, 1472 (1968).
[14]H. R. Child and W. C. Koehler, Appl. Phys. 40, 1274 (1970).

PHYSICAL REVIEW B VOLUME 2, NUMBER 7 1 OCTOBER 1970

Metallic Alloys and Exchange-Enhanced Paramagnetism. Application to Rare-Earth–Cobalt Alloys

D. Bloch and R. Lemaire
Laboratoire d'Electrostatique et de Physique du Métal,
Centre National de la Recherche Scientifique, 38-Grenoble-Gare, France
(Received 30 March 1970)

A phenomenological theory is presented of the magnetic properties of two-component alloys, one of whose components has a permanent magnetic moment, and the other an exchange-enhanced paramagnetic susceptibility. The paramagnetic susceptibility, magnetic-ordering temperature, and magnetization at low temperature are discussed in terms of this theory, and the results obtained are applied to cubic alloys ACo_2 between rare earth (A) and cobalt.

INTRODUCTION

The behavior of intermetallic alloys between rare earths and transition metals is often complex.[1] Cobalt does not possess a magnetic moment in YCo_2 or $LuCo_2$. In the alloys with magnetic rare earths, the magnetic moment of cobalt varies with the spin of the rare earth. In $GdCo_2$ or $TbCo_2$, the magnetic moments of the rare-earth and cobalt atoms are antiparallel, whereas in $NdCo_2$ or $PrCo_2$ they are ferromagnetically aligned.[2]

We present a phenomenological theory for these alloys, and using this theory we study their paramagnetic susceptibility, magnetic-ordering temperature, and magnetization at low temperature.

I. MODEL AND ITS MAIN CONSEQUENCES

We consider an alloy formed with two types of atoms, A and B, located in two different crystallographic sites. We assume that A possesses a well-localized magnetic moment and that B gives rise, in the crystal, to electronic energy bands leading to an exchange-enhanced paramagnetic susceptibility. In the high-temperature range, the magne-